



Original Article



Proanthocyanidin Alleviates Liver Ischemia/Reperfusion Injury by Suppressing Autophagy and Apoptosis via the PPAR α /PGC1 α Signaling Pathway

Zhilu Yao^{1,2}, Ning Liu^{3*}, Hui Lin^{1*}  and Yingqun Zhou^{2,4*} 

¹Department of Gastroenterology, Jingan District Zhabei Central Hospital, Shanghai, China; ²Clinical Medical College of Shanghai Tenth People's Hospital, Nanjing Medical University, Nanjing, Jiangsu, China; ³Department of Gastroenterology, Changzhou Maternal and Child Health Hospital, Changzhou, Jiangsu, China; ⁴Department of Gastroenterology, Shanghai Tenth People's Hospital, Tongji University School of Medicine, Shanghai, China

Received: 15 February 2023 | Revised: 6 May 2023 | Accepted: 17 May 2023 | Published online: 17 July 2023

Abstract

Background and Aims: Hepatic ischemia-reperfusion injury (IRI) is a common pathophysiological phenomenon in clinical practice, which usually occurs in liver transplantation, liver resection, severe trauma, and hemorrhagic shock. Proanthocyanidin (PC), exerted from various plants with antioxidant, antitumor, and antiaging activity, were administered in our study to investigate the underlying mechanism of its protective function on IRI. **Methods:** Two doses of PC (50 mg/kg, 100 mg/kg) were given to BALB/c mice by intragastric administration for 7 days before partial (70%) warm IR surgery. Serum and liver tissues were collected 2, 8, and 24 h after reperfusion for relevant experiments. **Results:** The results of transaminase and hematoxylin and eosin staining indicated that PC pretreatment significantly alleviated IRI in mice. Serum total superoxide dismutase increased and malondialdehyde decreased in PC pretreatment groups. Enzyme-linked immunosorbent assays, western blotting, quantitative real-time polymerase chain reaction, and immunohistochemistry showed that inflammation, apoptosis, and autophagy in PC preprocessing groups were significantly inhibited and were dose-dependent. The protein, mRNA expression, and immunohistochemical staining results of peroxisome proliferator-activated receptor alpha (PPAR α) and peroxisome proliferator-activated receptor gamma coactivator 1-alpha (PGC1 α) in the PC pretreatment groups were significantly upregulated

compared with the IR group in a dose-dependent manner. **Conclusions:** PC pretreatment suppressed inflammation, apoptosis, and autophagy via the PPAR- α signaling pathway to protect against IRI of the liver in mice.

Citation of this article: Yao Z, Liu N, Lin H, Zhou Y. Proanthocyanidin Alleviates Liver Ischemia/Reperfusion Injury by Suppressing Autophagy and Apoptosis via the PPAR α /PGC1 α Signaling Pathway. J Clin Transl Hepatol 2023;11(6):1329–1340. doi: 10.14218/JCTH.2023.00071.

Introduction

Ischemia-reperfusion injury (IRI) refers to restoring the blood perfusion on the basis of ischemia, further aggravating the tissue damage caused by ischemia, and even causing irreversible damage.^{1–3} Severe hepatic IRI is responsible for graft rejection, liver dysfunction and graft failure after liver transplantation and hepatectomy.⁴ To attenuate the harmful effects of hepatic IRI, many studies introduce pharmacological interventions or invasive procedures and results show that pharmacological pretreatment (sevoflurane, propofol, sufentanil, and others), hepatic Inflow modulation (ischemic preconditioning, remote ischemic preconditioning, and pre-retrieval reperfusion), and machine perfusion (hypothermic perfusion, dual hypothermic perfusion, normothermic perfusion, and regional normothermic perfusion) modified injury and diminished the impact. However, clinical data are limited and there is no effective clinical treatment to prevent IRI.⁵ We established animal models to investigate the underlying mechanism and possible protective strategies.

Reactive oxygen species (ROS) in liver cells are maintained at baseline under normal physiologic conditions. When the liver suffers from IRI, liver cells produce excessive ROS, which in turn recruits and activates Kupffer cells.³ Activated Kupffer cells secrete proinflammatory and proapoptotic cytokines, which results in sterile inflammation and apoptosis.⁶ Autophagy is a survival mechanism of cells in a harsh environment, but persistent autophagy can lead to the occurrence of programmed cell death during IRI.⁷ Thus far, many animal studies have confirmed that pharmacologic pretreat-

Keywords: Liver ischemia/reperfusion injury; Proanthocyanidin; Apoptosis; Autophagy; PPAR α ; PGC1 α .

Abbreviations: ALT, alanine aminotransferase; AST, aspartate aminotransferase; HE, hematoxylin and eosin; IL-1 β , interleukin 1 beta; IRI, ischemia-reperfusion injury; MDA, malondialdehyde; NC, normal control; PC, proanthocyanidin; PGC-1 α , PPAR- γ coactivator 1 alpha; PPAR α , peroxisome proliferator-activated receptor alpha; qRT-PCR, quantitative real-time polymerase chain reaction; ROS, reactive oxygen species; TNF- α , tumor necrosis factor-alpha; T-SOD, total superoxide dismutase.

***Correspondence to:** Yingqun Zhou, Clinical Medical College of Shanghai Tenth People's Hospital, Nanjing Medical University, Nanjing, Jiangsu 211166, China. ORCID: <https://orcid.org/0000-0001-8757-9657>. Tel/Fax: +86-21-66300588, E-mail: yqzh02@163.com; Hui Lin, Department of Gastroenterology, Jingan District Zhabei Central Hospital, Shanghai 200072, China. ORCID: <https://orcid.org/0000-0002-7112-8752>. Tel: +86-21-56628584, Fax: +86-21-56316699, E-mail: niliuh@163.com; Ning Liu, Department of Gastroenterology, Changzhou Maternal and Child Health Hospital, Changzhou, Jiangsu 213004, China. Tel: +86-519-88581101, Fax: +86-519-88109879, E-mail: lnn10202@163.com

Table 1. Primary antibodies used for western blotting and immunohistochemical staining

Antibody	Species	Targeted species	Dilution ratio in western blotting	Supplier	Catalog number	Molecular weight in kDa
Bax	Rabbit	H, M, R	1:1,000	PT	23931-1-AP	21–24
Bcl-2	Rabbit	H, M, R	1:500	WLB	WL01556	26
Beclin-1	Rabbit	H, M, R	1:1,000	PT	11306-1-AP	60
IL-1 β	Mouse	H, M	1:1,000	CST	12242	17
PPAR- α	Rabbit	H, M, R	1:1,000	PT	15540-1-AP	52–55
TNF- α	Rabbit	M	1:1,000	CST	11948 s	17
PGC1 α	Rabbit	H, M, R	1:1,000	Abcam	Ab54481	92
Caspase-3	Rabbit	H, M, R	1:1,000	PT	19677-1-AP	17.32–35
LC3	Rabbit	H, M, R	1:1,000	PT	14600-1-AP	16–18
β -actin	Mouse	H, M, R	1:1,000	CST	3700	43

CST, Cell Signaling Technology (Danvers, MA, USA); H, human; M, mouse; PT, Proteintech (Chicago, IL, USA); R, rat; WLB, Wanleibio (Shenyang, China); IL-1 β , interleukin 1 beta; PGC-1 α , PPAR- γ coactivator 1 alpha; PPAR α , peroxisome proliferator-activated receptor alpha; TNF- α , tumor necrosis factor- α .

ment can reduce IRI. PC, a novel highly effective antioxidant, is a powerful free radical scavenger, and has anti-inflammatory and antitumor activity.^{8–10} Previous studies have shown that PC alleviated intestinal, heart, and kidney IRI.^{10–12} Furthermore, Xu *et al.*¹³ found that PC protected liver against IRI by attenuating endoplasmic reticulum stress. However, other potential mechanisms of the protective effect of PC on liver IRI have not been explored. Yang *et al.*¹⁴ reported that PC reversed the inhibition of the peroxisome proliferator-activated receptor alpha (PPAR α) signaling pathway and improved liver injury caused by lead intake. PPAR α , a nuclear receptor, is a therapeutic target for various metabolic diseases and also has anti-inflammatory and anti-apoptotic activity.^{15,16} Therefore, we speculated that PPAR α might protect the liver from IRI through the PPAR α signaling pathway. In this study, we demonstrated that PC alleviated liver IRI by suppressing autophagy and apoptosis through the PPAR α /PGC1 α signaling pathway, providing a new treatment strategy for liver IRI.

Methods

Reagents

The PC used in this study was purchased from Kingmorn industry, diluted in normal saline, and stored away from light at 4°C. GW6471, an antagonist of PPAR α , was purchased from MedChemExpress (Monmouth Junction, NJ, USA). Alanine aminotransferase (ALT) and aspartate aminotransferase (AST) microplate test kits, total superoxide dismutase (T-SOD) assay kits (hydroxylamine method), and malondialdehyde (MDA) assay kits (thiobarbituric acid method) were purchased from the Nanjing Jiancheng Bioengineering Institute (Jiancheng Biotech, China). Tumor necrosis factor- α (TNF- α) and interleukin 1 beta (IL-1 β) ELISA kits were acquired from eBioscience (San Diego, CA, USA). RNA quantitative real-time polymerase chain reaction (qRT-PCR) kits were obtained from Takara Biotechnology (Dalian, China). The primary antibodies used in this study are shown in Table 1. Antirabbit or antimouse secondary antibodies were obtained from Dako (Santa Clara, CA, USA).

Animals

Seven-week-old male Balb/c mice weighting 20–25 g were purchased from Shanghai SLAC Laboratory Animal Co. Ltd (Shanghai, China), housed in plastic cages, and maintained

in an alternating 12 h:12 h light:dark cycle at a constant temperature (22–25°C) with free access to food and water. Mice were fed with normal food and water for 2 weeks to adapt to the environment. All animal experiments were consistent with National Institutes of Health Guidelines and were approved by the Animal Care and Use Committee of Shanghai Tongji University.

Experimental design

We used two doses of PC to investigate its effects on liver IRI as previously described.^{12,13} Eighty-four mice were randomly divided into six groups: (1) A normal control (NC) group of six mice given saline by gavage; (2) A PC group of six mice given 100 mg/kg PC by gavage for 7 days; (3) A sham group of 18 mice with laparotomy without IR surgery; (4) A group of 18 mice with IR surgery; (5) An IR+PC group of 18 mice given 50 mg/kg PC by gavage for 7 days before they underwent IR surgery; (6) An IR+PC (100 mg/kg) group of 18 mice given 100 mg/kg PC by gavage for 7 days before they underwent IR surgery.

Mice in groups one and two were sacrificed by cervical dislocation after 7 days of drug administration. Six mice in groups three to six were randomly sacrificed by cervical dislocation 2, 8, and 24 h after reperfusion.¹⁷ Orbital blood and middle and left liver lobes were gathered for experiments to determine whether PPAR α was associated with the protective effects of PC on liver IRI. Thirty mice were randomly divided into four groups, and we used GW6471 following the manufacturer's protocol.¹⁸ (1) A sham group of six mice received a laparotomy without IR surgery; (2) An IR+PC group of six mice were given 100 mg/kg PC by gavage for 7 days before IR surgery; (3) An IR+GW6471 group of six mice were given 20 mg/kg GW6471 by gavage for 7 days before IR surgery; (4) An IR+PC group of six mice given 20 mg/kg GW6471 and 100 mg/kg PC by gavage for 7 days before IR surgery.

Induction of a mouse IR model

We followed the methods of Deng *et al.*¹⁷ The mice were fasted 12 h before surgery and had free access to drinking water. Mice were anesthetized by intraperitoneal injection of 1.25% sodium pentobarbital (Nembutal; Sigma-Aldrich, St. Louis, MO, USA) at a dose of 40 mg/kg. After successful anesthesia, the mice were positioned flat on the operating table, their limbs were fixed with tape, and the operation area was disinfected with 75% ethanol. After making a 1 cm midline inci-

sion, the abdominal cavity was opened and the hepatic pedicles of the left and middle lobes of the liver were carefully separated (the portal vein and hepatic artery supplying blood to the left and middle lobes of the liver). The portal vein and hepatic artery of the middle and left lobes were clamped with a noninvasive vascular clip to establish 70% liver ischemia model that prevented severe mesenteric venous congestion. Compared with the nonblocked right lobe, the blocked lobes became gray, indicating that blocking was successful. The abdomen was covered with gauze soaked in saline and the mice were placed on a heating pad at a constant temperature of 37°C. After 45 m of continuous ischemia, the vascular clip was removed to restore the ischemic liver blood flow. The liver in the ischemic area gradually returned to red from gray, indicating successful reperfusion. The abdominal muscles and skin layers were sutured to close the abdominal cavity.

Biochemical analysis

After incubating at 4°C for 6 h, collected blood samples were centrifuged at 4,600 rpm for 10 m to separate serum and stored at -80°C. Serum ALT, AST, MDA, T-SOD were assayed by test kits following the manufacturer's protocols. Serum TNF- α and IL-1 β were measured by ELISA kits following the manufacturer's protocols.

Hematoxylin and eosin (HE) staining

Tissues from the left lobe of the liver were collected and fixed in 4% paraformaldehyde for at least 24 h. The fixed tissues were dehydrated in different concentrations of alcohol and cleared with xylene before being embedded in paraffin, sectioned at 4 μ m, and stained with HE. Histopathological damage was observed by light microscopy.

qRT-PCR

qRT-PCR was performed as described by Feng *et al.*¹⁹ TRIzol (Thermo Fisher Scientific, Waltham, MA, USA) was used to extract total RNA from the left liver lobe. After determining the RNA concentration, samples were reverse transcribed to cDNA using a reverse transcription kit (Takara Biotechnology, Beijing, China). Gene expression at the mRNA level was detected by SYBR Green qRT-PCR with a 7900HT fast RT-PCR system (Applied Biosystems, Foster City, CA, USA). The primers used in this study are shown in Table 2. The specificity of primers was verified by Sanger sequencing of the amplified PCR products. The relative mRNA expression levels were determined by the 2^{- $\Delta\Delta$ Ct} method and normalized against β -actin.

Western blotting

Western blotting was performed as described by Xu *et al.*⁴ Fresh liver was cut into small pieces, frozen in liquid nitrogen, and stored at -80°C. The tissues were ground into powder at a low temperature (dipped in liquid nitrogen), and RIPA buffer (along with protease inhibitors) was used to extract the proteins. The protein concentration was determined by the bicinchoninic acid method, the sample was mixed with 5 \times loading buffer, heated at 100°C for 10 m, and then store at -20°C. Proteins of different molecular weights were separated by 10% or 12.5% sodium dodecyl-sulfate polyacrylamide gel electrophoresis and transferred to polyvinylidene fluoride membranes. After blocking in 5% skim milk diluted in PBS for at least 1 h, the membranes were incubated at 4°C overnight with anti-TNF- α , -IL-1 β , - β -actin, -Bcl-2, -Bax, -Beclin-1, -caspase3, -LC3, -PPAR α , and -PGC1 α primary antibodies. The membrane was eluted three times with PBS including 0.1% Tween-20 before applying secondary antibodies for 1 h in

Table 2. Primers for real-time polymerase chain reaction assays

Target gene	Designed primer sequence (5'→3')
β -actin	Forward GGCTGTATTCCCCTCCATCG
	Reverse CCAGTTGGTAAACAATGCCATGT
IL-1 β	Forward GAAATGCCACCTTTTGACAGTG
	Reverse TGGATGCTCTCATCAGGACAG
TNF- α	Forward CAGGCGGTGCCTATGTCTC
	Reverse CGATCACCCCGAAGTTCAGTAG
Beclin1	Forward ATGGAGGGGTCTAAGGCGTC
	Reverse TGGGCTGTGGTAAGTAATGGA
Bcl-2	Forward GCTACCGTCGTGACTTCGC
	Reverse CCCACCGAACTCAAAGAAGG
Bax	Forward AGACAGGGGCCCTTTTGCTAC
	Reverse AATTCGCCGAGACTCG
Caspase-3	Forward CTCGCTCTGGTACGGATGTG
	Reverse TCCCATAAATGACCCCTTCATCA
LC3	Forward TTATAGAGCGATACAAGGGGGAG
	Reverse CGCCGTCTGATTATCTTGATGAG
PGC1 α	Forward TGATGACAGCGAAGATGAAAGTG
	Reverse TTTGGGTGGTGACACGGAAT
PPAR α	Forward AACATCGAGTGTCTGAATATGTGG
	Reverse CCGAATAGTTCGCCGAAAGAA

IL-1 β , interleukin 1 beta; PGC-1 α , PPAR- γ coactivator 1 alpha; PPAR α , peroxisome proliferator-activated receptor alpha; TNF- α , tumor necrosis factor-alpha.

the dark at room temperature. An Odyssey two-color infrared laser imaging system (LI-COR Biosciences, Lincoln, NE, USA) was used to detect excited fluorescent signals from the membranes.

Immunohistochemical staining

We followed the methods described by Wang *et al.*²⁰ Tissue slices obtained 8 h after reperfusion were baked in an oven at 60°C for 2 h. After dewaxing and rehydration, sections were dipped in citrate buffer and incubated in a water bath at 90°C for 20 m to achieve antigen retrieval. The sections were washed with 3% hydrogen peroxide to prevent endogenous catalase activity and blocked with 5% bovine serum albumen for 20 m to block nonspecific staining. The sections were incubated at 4°C overnight with anti-TNF- α , -IL-1 β , -Bcl-2, -Bax, -LC3 (all 1:200); anti-PPAR α , -anti-PGC1 α (all 1:100), and anti-Beclin-1 (1:500) primary antibodies. Secondary antibodies were added with incubation at 37°C for 1 h. After counter-staining with diaminobenzidine, the sections were observed by light microscopy.

Terminal deoxynucleotidyl transferase dUTP nick end labeling (TUNEL)

After dewaxing and rehydration, tissue sections were treated with proteinase K to increase the permeability of the cell and nuclear membranes, and the TUNEL reaction mixture was added. The results were observed by light microscopy.

Statistical analysis

Data were reported as means \pm SD and all experiments were

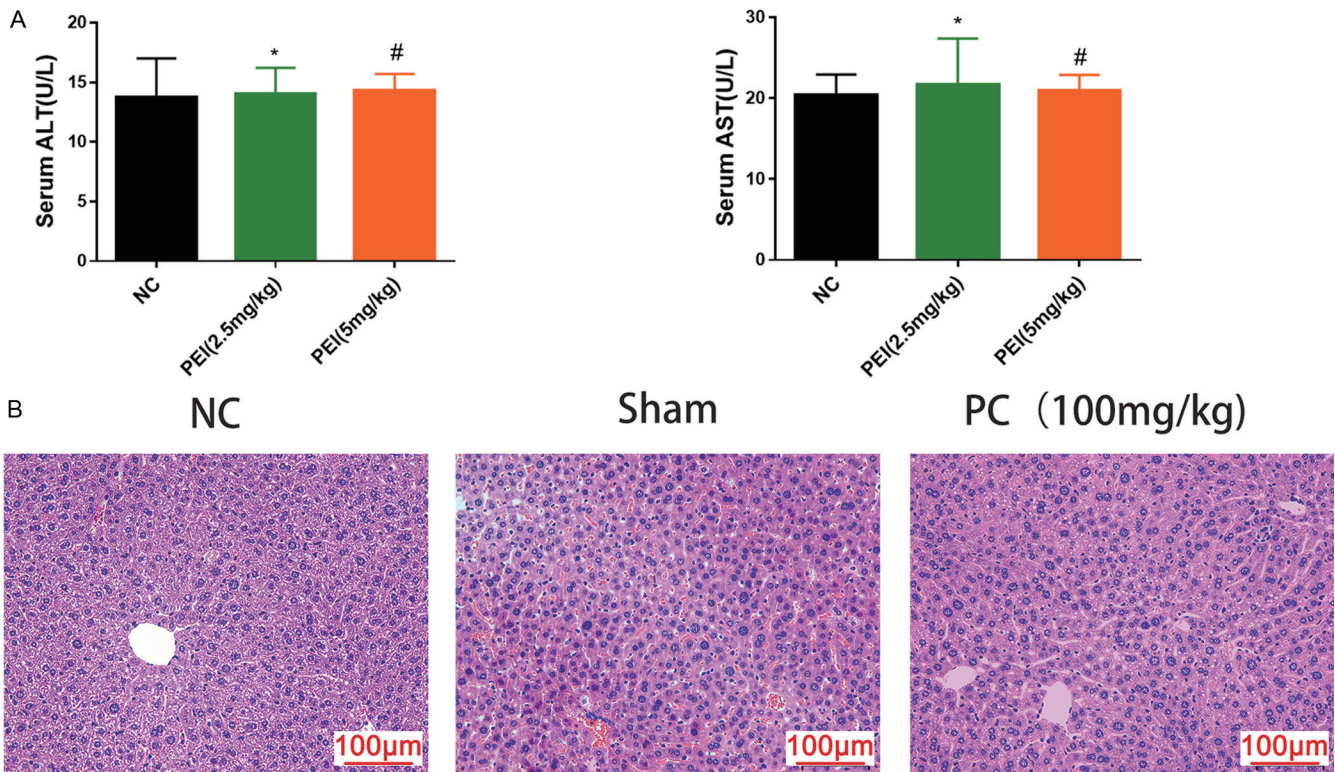


Fig. 1. PC had no harm on liver structure or function. (A) Serum ALT and AST levels are means±SDs ($n=6$; $p>0.05$). (B) Representative hematoxylin and eosin-stained hepatic sections were examined under light microscopy and imaged at a 200× magnification. ALT, alanine aminotransferase; AST, aspartate aminotransferase; IR, ischemia-reperfusion; NC, normal control; PC, proanthocyanidin.

repeated at least three times. Serum ALT, AST, T-SOD, and MDA assay, ELISA, and qRT-PCR results were analyzed with Student's *t*-tests. *P*-values<0.05 were considered statistically significant, and statistical figures were drawn by GraphPad Prism 6 (GraphPad Software, Inc., San Diego, CA, USA).

Results

PC administration alone had no effect on liver function

To determine whether PC was hepatotoxic, we tested serum AST and ALT levels in the NC, sham and PC (100 mg/kg) groups, and the results were not statistically different (Fig. 1A). Histological evaluation of HE stained tissue consistently found no obvious tissue damage (Fig. 1B). The results indicated that PC administration alone had no effect on liver function.

PC pretreatment alleviated hepatic IRI in mice

Pathological changes of liver tissues were observed by light microscopy. In contrast to the sham group, large areas of necrosis, extensive congestion, and the formation of large numbers of vacuoles were observed in the IR group. The damage was reduced in IR+PC group (most relieved in high dose group) (Fig. 2A, B). We determined serum AST and ALT at three times (2, 8, and 24 h after reperfusion). The results showed that ALT and AST were significantly higher in the IR group than in the sham operation group and the levels of the pretreated groups were significantly decreased in a dose-dependent manner (Fig. 2C). In conclusion, PC pretreatment alleviated IRI liver injury.

PC preconditioning suppressed oxidative stress

During IRI, large amounts of ROS accumulated in hepatic cells, causing oxidative stress. We detected serum T-SOD (a major antioxidant metalloenzyme) and MDA (one of the final products of membrane lipid peroxidation). Compared with the IR group, the serum T-SOD of PC groups significantly increased and the serum MDA were increased (Fig. 3A).

PC pretreatment inhibited the release of inflammatory cytokines including IL1-β and TNF-α

Inflammation is of vital importance in IRI. IL-1β and TNF-α, as major inflammatory cytokines, were tested by ELISA, qRT-PCR, western blotting, and immunohistochemical staining (Fig. 3B-E). Serum IL-1β and TNF-α levels, protein and mRNA expression extremely increased in the IR group, and were ameliorated by PC in the preprocessing groups. IR+PC (100 mg/kg) group demonstrated a massive decline in inflammatory cytokines compared with IR+PC (50 mg/kg) group. In summary, PC inhibited the release of inflammatory cytokines and had a significant dose-dependent property.

PC pretreatment attenuated hepatocyte apoptosis and autophagy during hepatic IRI in mice

Autophagy and apoptosis, two kinds of programmed cell death, are responsible for liver dysfunction and a suboptimal clinical prognosis. Bax, Bcl-2, caspase3, LC3, and Beclin-1 were examined to assess the specific changes of autophagy and apoptosis in each group. Results of western blotting, qRT-PCR, and immunohistochemical staining showed that IR activated Bax, Beclin-1, caspase3, and LC3 and inhibited Bcl-2. On the contrary, PC administration downregulated Bax,

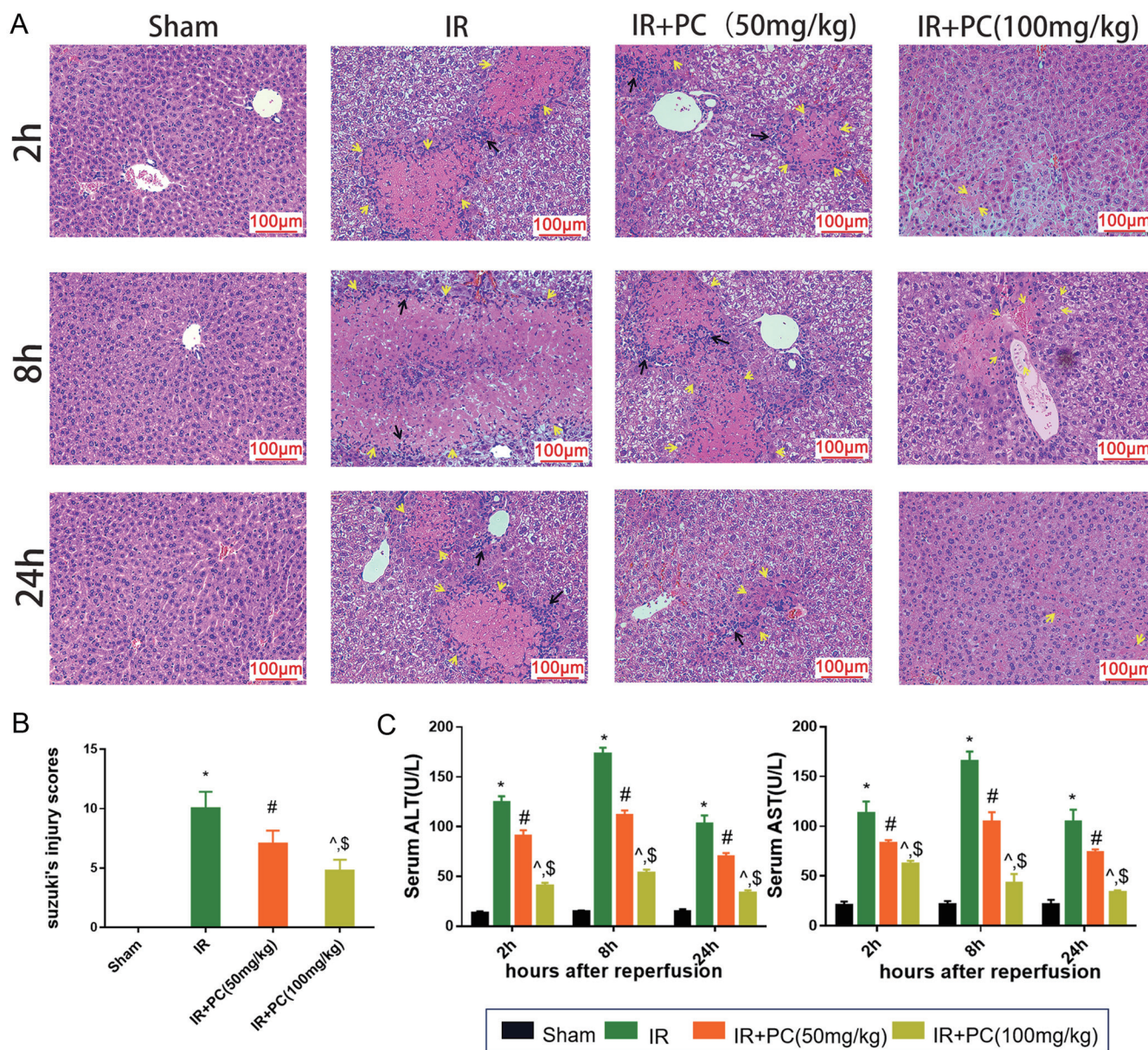


Fig. 2. PC pretreatment ameliorated hepatic IRI in mice. (A) Representative hematoxylin and eosin-stained hepatic sections were examined by light microscopy and imaged at 200× magnification. Yellow arrows show necrosis and black arrows show inflammatory cells. (B) Suzuki's pathological criteria were used to determine the degree of liver injury at 8 h post-reperfusion. (C) Serum ALT and AST levels. Data are means±SDs (n=6; *p<0.05 for IR vs. sham; #p<0.05 for IR+PCs (50 mg/kg) vs. IR; ^p<0.05 for IR+PCs (100 mg/kg) vs. IR; \$p<0.05 for IR+PCs (50 mg/kg) vs. IR+PCs (100 mg/kg). ALT, alanine aminotransferase; AST, aspartate aminotransferase; IR, ischemia-reperfusion; NC, normal control; PC, proanthocyanidin.

caspase3, LC3 and Beclin-1 expression and upregulated Bcl-2 (Fig. 4A–C). In a word, PC pretreatment relieved hepatocyte apoptosis and autophagy during hepatic IRI in mice.

PC activated PPARα signaling in hepatic IRI

In summary, PC protected liver from IRI by inhibiting oxidative stress, inflammation, apoptosis, and autophagy, but the underlying molecular mechanism was not determined. PGC1α, a coactivator of PPARγ that suppressed Bax and up-regulated bcl2²¹ has multiple interactions with PPARα.^{22–24} Therefore, we detected the protein and mRNA levels of

PPARα and PGC1α. The results showed that both PPARα and PGC1α expression were significantly higher in PC pretreatment groups than in the IR group (Fig. 5A, B) and were consistent with the results of immunohistochemical staining pictures (Fig. 5C). Therefore, PC activated the PPARα/PGC1α signaling pathway.

PC protected mice from liver IRI through PPARα

To further determine whether PPARα was involved in the protection of PC against liver IRI, we investigated the effects of GW6471, a selective antagonist of PPARα. As shown in

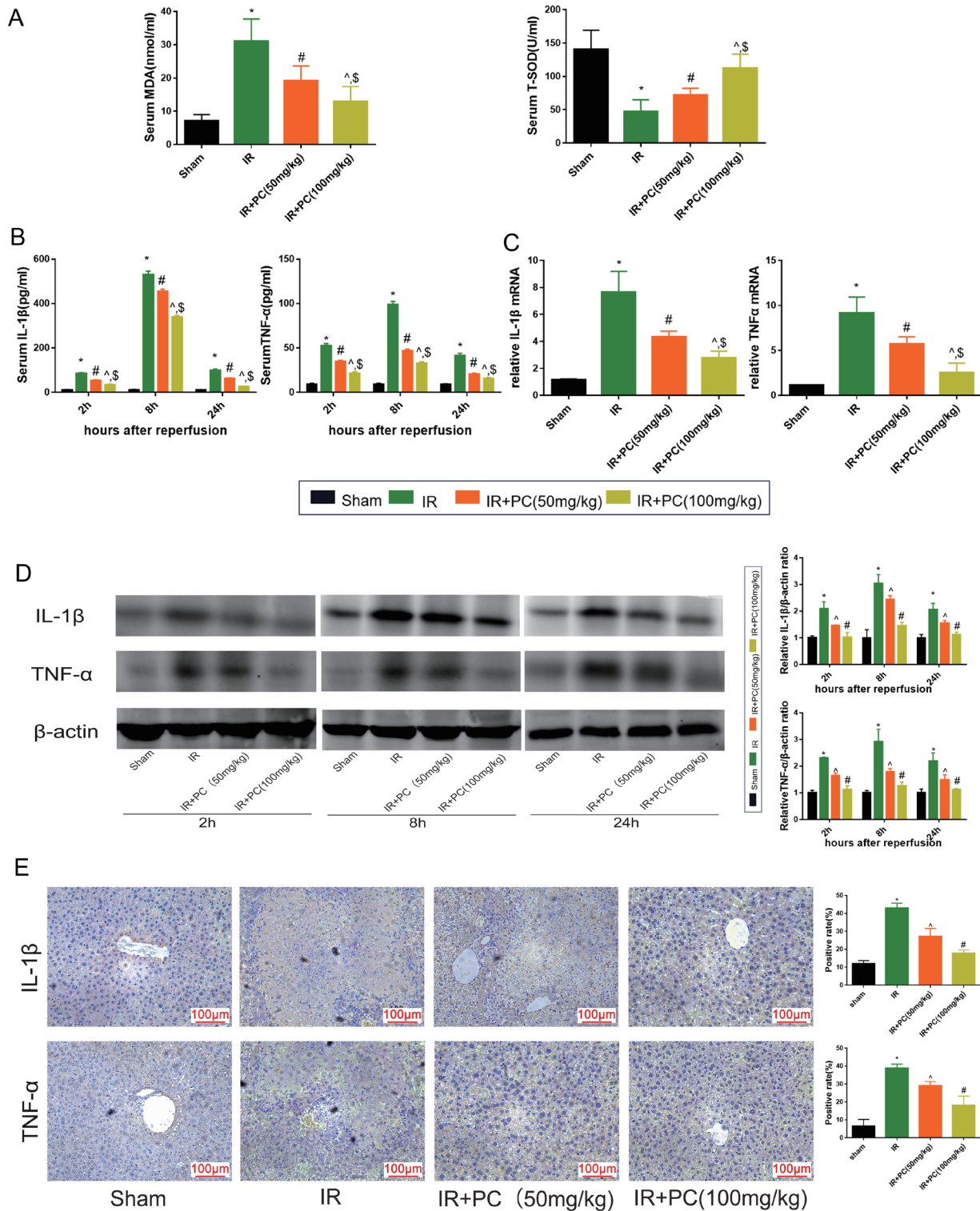


Fig. 3. PC pretreatment alleviated oxidative stress and inhibited the release of inflammatory cytokines including IL-1β and TNF-α. (A) Serum T-SOD and MDA levels. (B) Serum TNF-α and IL-1β were detected by ELISA. (C) Relative TNF-α and IL-1β mRNA levels in liver tissues at 8 h after reperfusion were determined by qRT-PCR. (D) Western blot assays of TNF-α and IL-1β protein levels. Relative gray values were calculated by ImageJ. (E) Representative TNF-α and IL-1β protein expressions in liver tissues at 8 h after reperfusion are shown by immunohistochemical staining and observed under microscopy and imaged at 200× magnification. ImageJ was used to calculate the positive rate. Data are means±SDs (n=6; *p<0.05 for IR vs. sham; #p<0.05 for IR+PCs (50 mg/kg) vs. IR; ^p<0.05 for IR+PCs (100 mg/kg) vs. IR; \$p<0.05 for IR+PCs (50 mg/kg) vs. IR+PCs (100 mg/kg). IL-1β, interleukin-1β; IR, ischemia-reperfusion; MDA, malondialdehyde; PC, proanthocyanidin; qRT-PCR, quantitative real-time polymerase chain reaction; TNF-α, tumor necrosis factor-alpha; T-SOD, total superoxide dismutase.

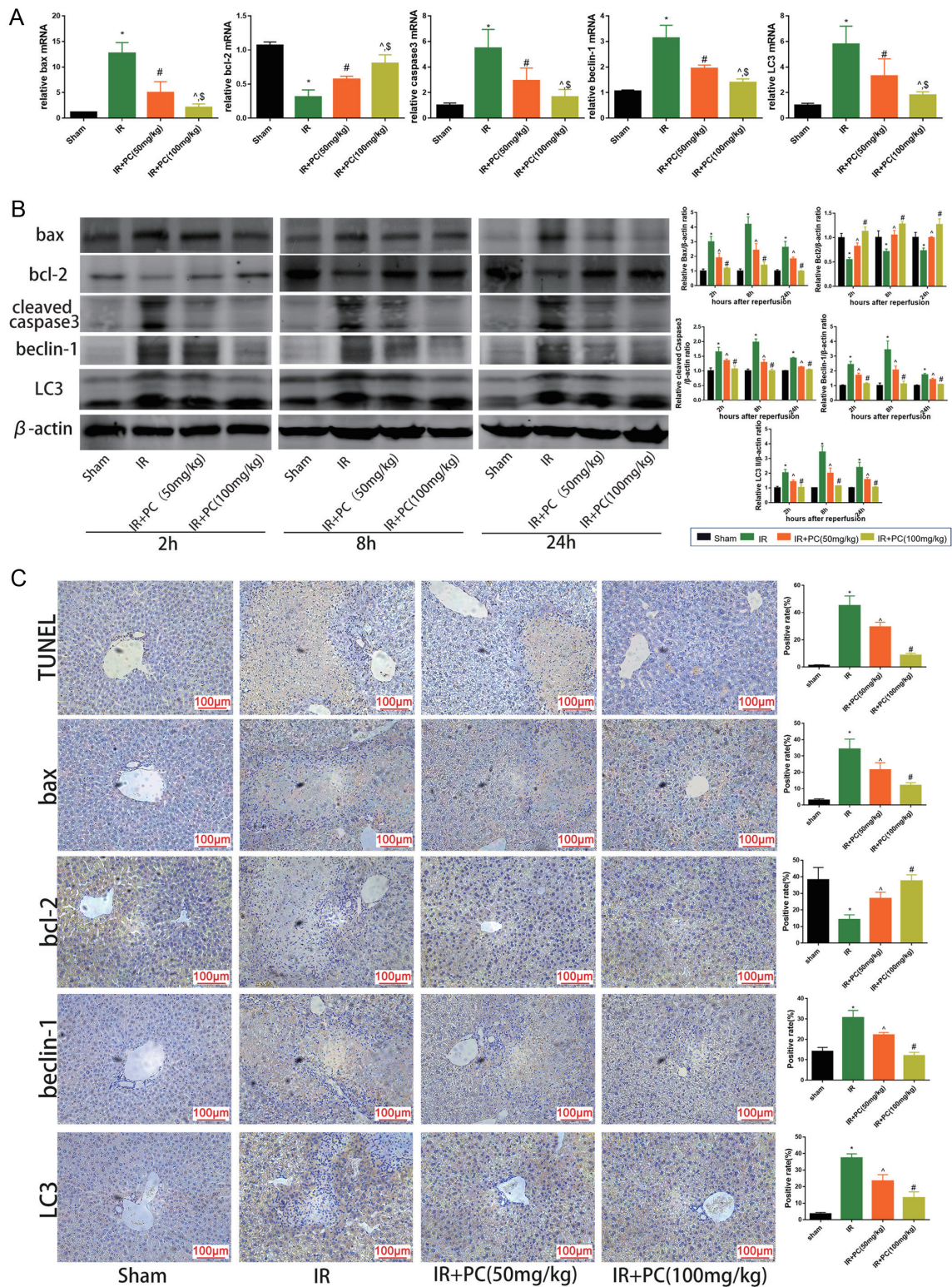


Fig. 4. PC pretreatment attenuated hepatocyte apoptosis and autophagy during hepatic IRI in mice. (A) Relative Bax, Bcl-2, caspase 3, beclin-1, and LC3 mRNA levels in liver tissue at 8 h after reperfusion were determined by qRT-PCR. (B) Western blots of Bax, Bcl-2, caspase3, beclin-1, and LC3 protein levels. Relative gray values were calculated by ImageJ. (C) TUNEL staining, Bax, Bcl-2, and beclin-1 protein expression in liver tissue at 8 h post-reperfusion are shown by immunohistochemical staining. ImageJ was used to calculate the positive rate. Data are means \pm SDs ($n=6$; * $p<0.05$ for IR vs. sham; # $p<0.05$ for IR+PCs (50 mg/kg) vs. IR; $\Delta p<0.05$ for IR+PCs (100 mg/kg) vs. IR; $\S p<0.05$ for IR+PCs (50 mg/kg) vs. IR+PCs (100 mg/kg). IR, ischemia-reperfusion; PC, proanthocyanidin; qRT-PCR, quantitative real-time polymerase chain reaction.

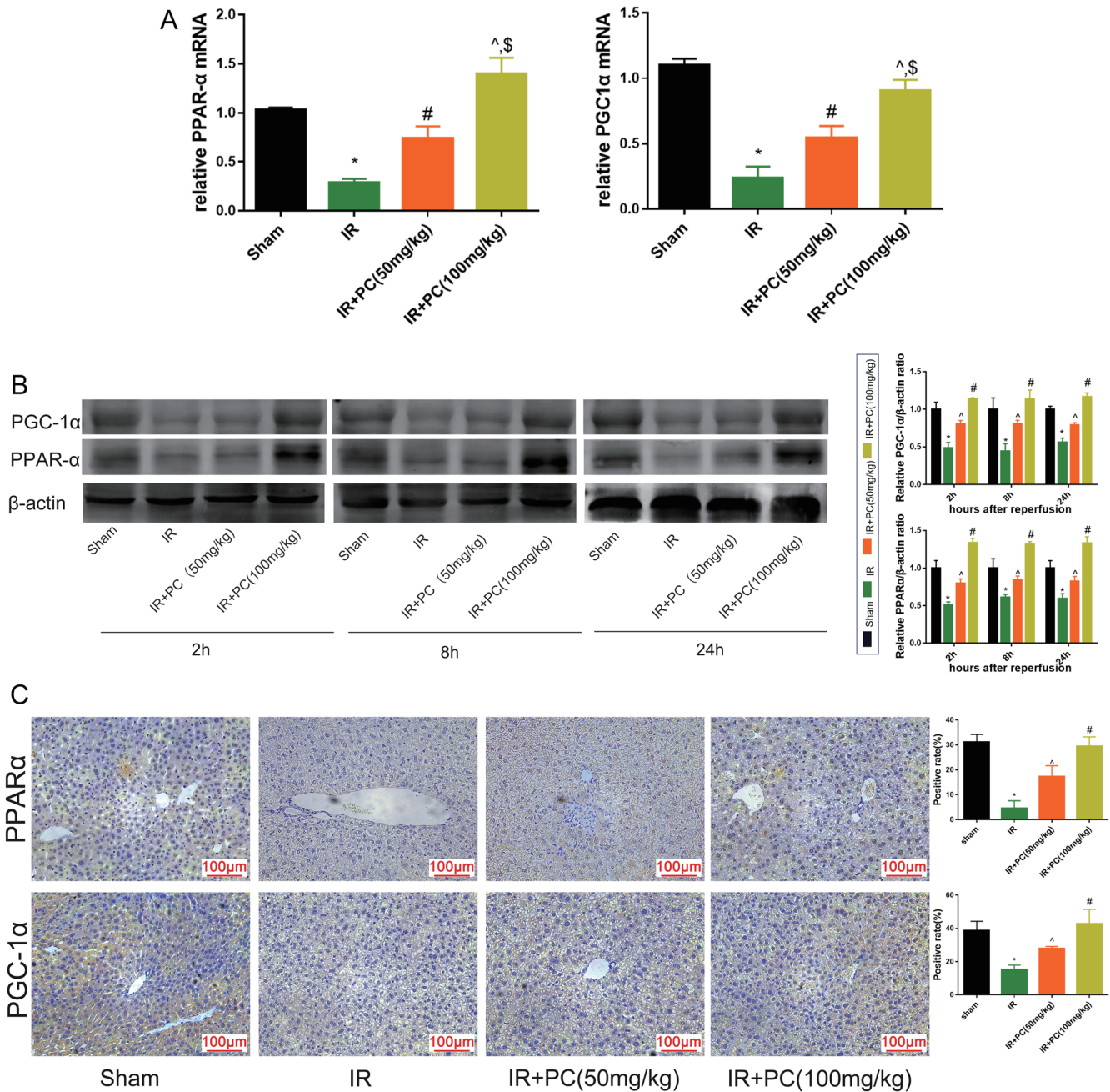


Fig. 5. PC activated PPAR-α signaling in hepatic IRI and probable mechanisms of PCs preconditioning against hepatic IR injury. (A) Relative PPARα and PGC1α mRNA levels in liver tissues at 8 h after reperfusion were determined by qRT-PCR. (B) Western blots of PPARα and PGC1α protein levels. Relative gray values were calculated by ImageJ. (C) PPARα and PGC1α protein expression in liver tissue at 8 h post-reperfusion are shown by immunohistochemical staining. ImageJ was used to calculate the positive rate. Data are means±SDs (n=6; *p<0.05 for IR vs. sham; #p<0.05 for IR+PCs (50 mg/kg) vs. IR; [^]p<0.05 for IR+PCs (100 mg/kg) vs. IR; ^{\$}p<0.05 for IR+PCs (50 mg/kg) vs. IR+PCs (100 mg/kg). IR, ischemia-reperfusion; qRT-PCR, quantitative real-time polymerase chain reaction; PC, proanthocyanidin; PGC1α, peroxisome proliferator-activated receptor gamma coactivator 1-alpha; PPARα, peroxisome proliferator-activated receptor alpha.

Figure 6A, the serum T-SOD level was lower in GW6471(20 mg/kg) + IR group than in other groups. PC (100 mg/kg) + GW6471 + IR improved the decline. The levels of ALT and ALT in GW6471 (20 mg/kg) + IR group were the highest, while those in PC (100 mg/kg) + GW6471 + IR group were decreased (Fig. 6B). HE staining of GW6471 (20 mg/kg) + IR group tissue demonstrated largest area of necrosis, and cotreatment with PC (100 mg/kg) alleviated liver injury (Fig.

6C). Protein expression of IL-1β, TNF-α, Bax, caspase3, beclin-1, LC3 of GW6471 (20 mg/kg) + IR group is obviously higher than other four groups, but introduction of PC (100 mg/kg) reversed the elevation. However, the expression of Bcl-2, PPARα and PGC1α were downregulated in GW6471 (20 mg/kg) + IR group and were reversed by PC (100 mg/kg) (Fig. 6D, E). All the results indicated that the inhibition of PPARα by GW6471 aggravated liver IRI, and PC reversed the

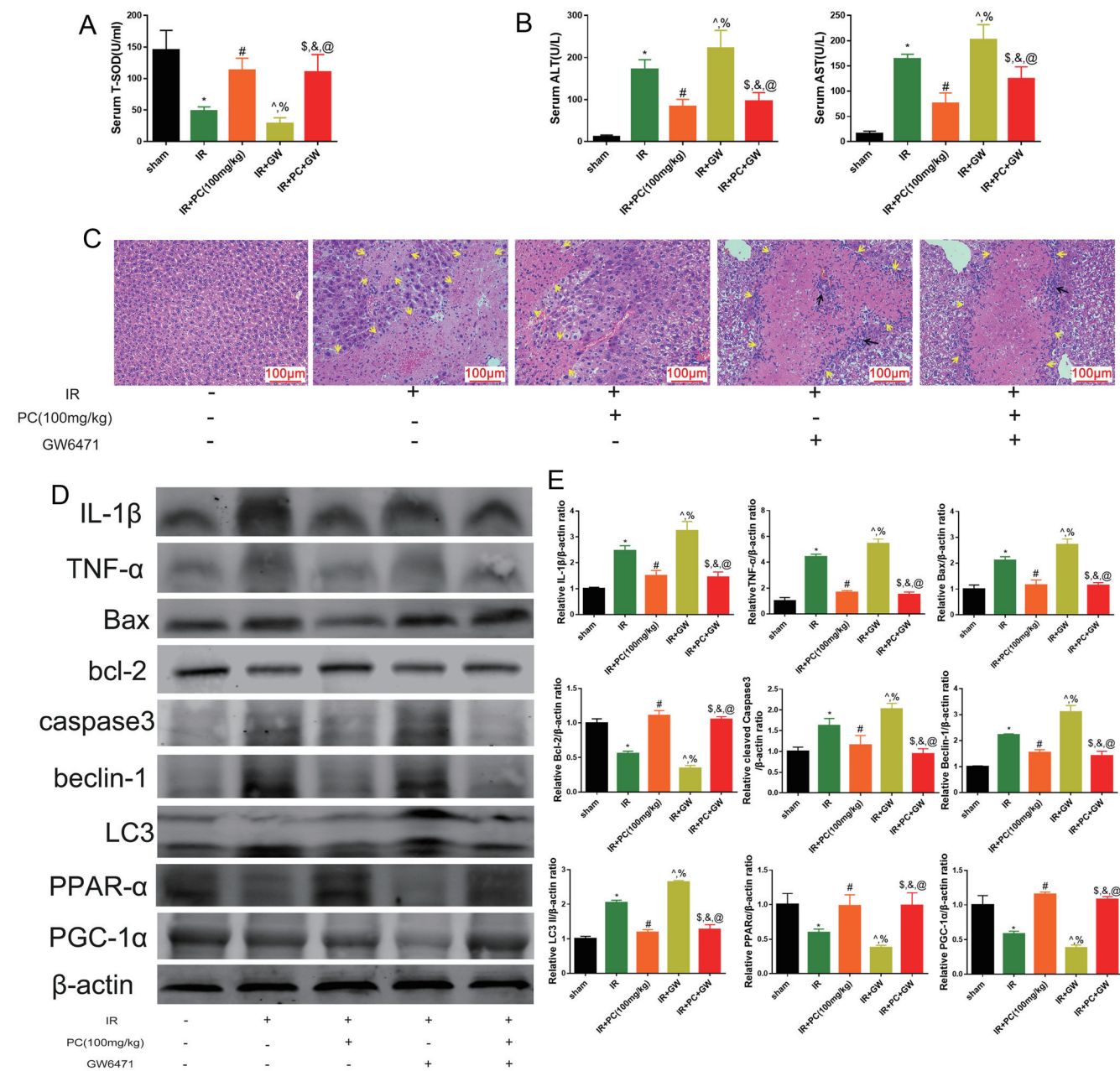


Fig. 6. PC protected mice from liver ischemia-reperfusion injury through PPARα. (A) Serum T-SOD levels. (B) Serum ALT and AST levels. (C) Representative hematoxylin and eosin-stained hepatic sections 8 h after reperfusion were examined by light microscopy and imaged at 200× magnification. Yellow arrows show necrosis and black arrows shows inflammatory cells. (D–E) Western blots of TNF-α, IL-1β, Bax, Bcl-2, caspase3, beclin-1, LC3, PPARα, PGC1α protein levels. Data are means±SDs (n=6; *p<0.05 for IR vs. sham; #p<0.05 for IR+PCs (100 mg/kg) vs. IR; ^p<0.05 for IR+GW6471 (20 mg/kg) vs. IR; \$p<0.05 for IR+PC (100 mg/kg)+GW6471 (20 mg/kg) vs. IR; %p<0.05 for IR+PC (100 mg/kg) vs. IR+GW6471 (20 mg/kg); &p>0.05 for IR+PC (100 mg/kg) vs. IR+PC (100 mg/kg)+GW6471 (20 mg/kg); @p<0.05 for IR+GW6471 (20 mg/kg) vs. IR+PC (100 mg/kg)+GW6471 (20 mg/kg). ALT, alanine aminotransferase; AST, aspartate aminotransferase; GW, GW6471; IL-1β, interleukin-1β; IR, ischemia-reperfusion; PC, proanthocyanidin; PGC1α, peroxisome proliferator-activated receptor gamma coactivator 1-alpha; PPARα, peroxisome proliferator-activated receptor alpha; TNF-α, tumor necrosis factor-alpha; T-SOD, total superoxide dismutase.

change. In conclusion, PPARα was associated with the protective effect of PC on IRI.

Discussion

Liver IRI has an important role in a variety of clinical adverse events, including graft rejection, liver dysfunction, and graft failure, which are a threat to liver transplantation and hepa-

tectomy patients.^{2,25} However, no effective clinical treatment has been used in liver IRI, and the underlying mechanism is still unclear. In-depth studies should be conducted to reveal the underlying mechanism and to develop novel treatments. Liver IRI can be divided into two stages, ischemia and reperfusion. During the ischemic phase, liver cells produce only a small amount of ROS. When liver blood perfusion is restored, ROS increases drastically owing to the massive transfer of

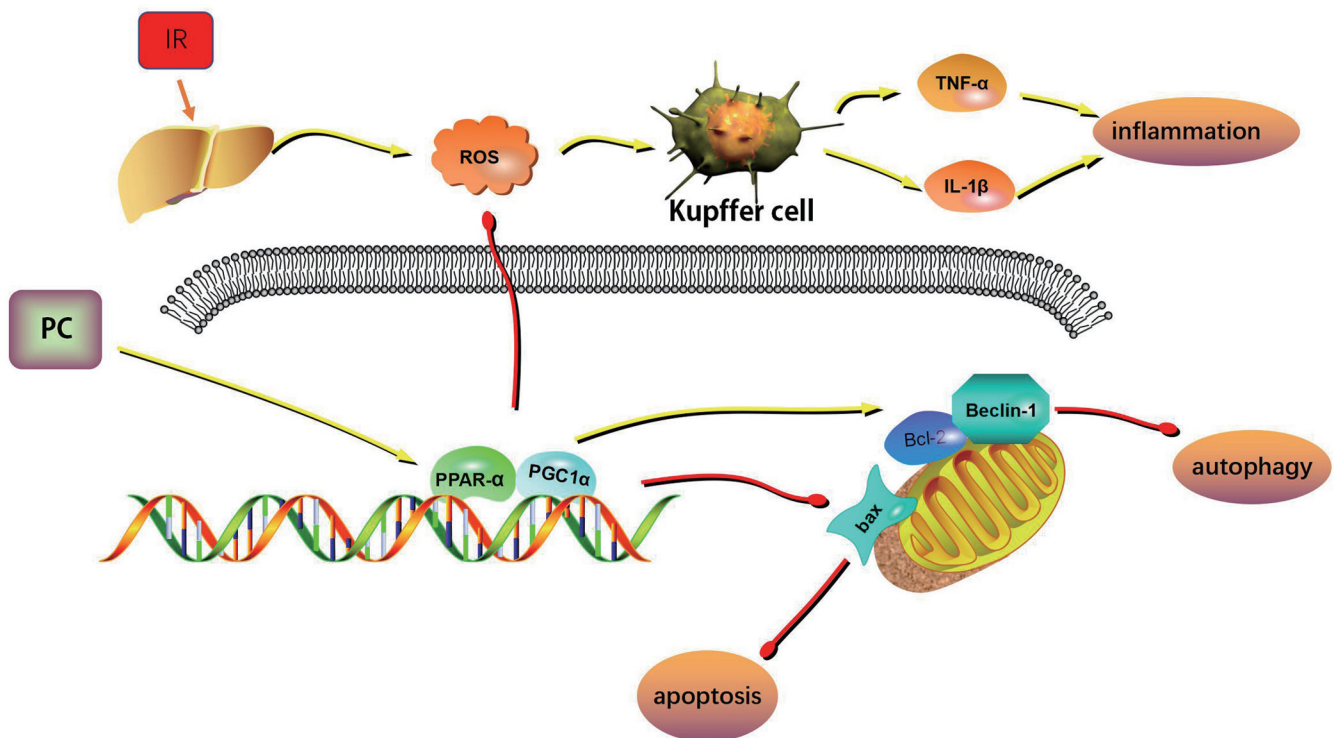


Fig. 7. PC pretreatment reduced liver IRI by suppressing autophagy and apoptosis by activating PPARα/PGC1α signaling pathway. IL-1β, interleukin-1β; IR, ischemia-reperfusion; PC, proanthocyanidin; PGC1α, peroxisome proliferator-activated receptor gamma coactivator 1-alpha; PPARα, peroxisome proliferator-activated receptor alpha; ROS, reactive oxide species; TNF-α, tumor necrosis factor-alpha.

electrons from electron carrier molecules in the mitochondria to oxygen,²⁶ thereby promoting apoptosis and autophagy. In addition, excessive ROS activates Kupffer cells, which then release additional proinflammatory and proapoptotic cytokines while producing more ROS, which aggravates liver damage.²⁷⁻²⁹ Accumulating ROS attacking the mitochondrial membrane leads to increased mitochondrial permeability, which results in cell damage.

PC is a strong, recently discovered antioxidant with potent anti-inflammatory and antitumor biological activity. PC exerts cardioprotective, neuroprotective, immunomodulatory, antidiabetic, anticancer, and antimicrobial activity through multiple pathway signalling.⁹ Furthermore, studies have shown that PC reduced IRI of the myocardium, kidney, and other organs.³⁰⁻³² Therefore, we speculated that PC can protect against liver IRI. By blocking the blood flow of the portal vein and part of the hepatic artery and restoring blood perfusion to the liver, we established a 70% liver warm IR model to explore the protective mechanism of PC against liver IRI. The study results demonstrated that PC pretreatment relieved hepatic damage in a dose-dependent manner.

PPARα belongs to the nuclear receptor superfamily and is a ligand-induced transcription factor with vital roles in glucose and lipid metabolism.^{33,34} PPARα also has anti-inflammatory and anti-oxidative stress properties.^{35,36} PGC1α is a transcriptional coactivator that functionally interacts with transcription factors to promote transcription of target genes.³⁷⁻³⁹ Through interaction with various transcription factors, PGC1α increases oxidative metabolism, mitochondrial biogenesis, and angiogenesis and reduces oxidative stress, and inflammation.⁴⁰ PPARα binds to the LXXL motif of PGC1α located in the N-terminal domain to form a PPARα/PGC1α complex.⁴¹ The PPARα/PGC1α complex promotes the expression of anti-

oxidant enzymes such as superoxide dismutase, which inhibit ROS and reduce liver damage.^{23,42-44} Additionally, decreased ROS inhibited Kupffer cell activation thereby reducing inflammation. Tang *et al.*²¹ have shown that PPARα/PGC1α inhibited Bax and upregulated the expression of Bcl-2. According to our results, PC pretreatment activated PPARα and PGC1α. With the upregulation of PPARα/PGC1α, the expression of Bcl-2 was upregulated and the expression of Bax, caspase 3, beclin-1 and LC3 were suppressed, indicating that PC suppressed apoptosis and autophagy. The combination of antiapoptotic protein Bcl-2 and proapoptotic protein Bax reduces mitochondrial membrane permeability, thereby inhibiting the release of cytochrome C and apoptosis mediated by caspase3.^{45,46} On the other hand, Bcl-2 binding to the BH3 domain resulted in beclin-1 inactivation and autophagy inhibition. To further verify that proanthocyanidin pretreatment protected the liver from IRI through PPARα signaling pathway, we administered GW6471, a PPARα antagonist to Balb/c mice to inhibit PPARα signaling. Proanthocyanidin pretreatment reversed the damage induced by GW6471, indicating that PPARα was involved in the protection of proanthocyanidin against liver IRI.

Conclusions

In conclusion, PC pretreatment reduced liver IRI by suppressing autophagy and apoptosis by activating PPARα/PGC1α signaling pathway, providing a new potential therapeutic target for liver IRI. The mechanism is shown in Figure 7.

Acknowledgments

The authors would like to acknowledge the helpful comments on this paper received from the reviewers.

Funding

The work was supported by the Natural Science Foundation of Shanghai (19ZR1439900) and Changzhou Science and Technology Bureau (CJ20200086).

Conflict of interest

The authors declare that they have no conflict of interests related to this publication.

Author contributions

ZY and YZ designed the research. YZ and NL provided critical fundings. ZY performed the research and analyzed results. ZY and HL wrote the paper. HL and YZ edited the manuscript and provided critical comments. All authors have made a significant contribution to this study and have approved the final manuscript.

Ethical statement

All animal protocols complied with the rules of the ethics committee of Shanghai Tenth People's Hospital (SH-DSYY-2022-1474).

Data sharing statement

The data used to support the findings of this study are available upon reasonable request from the corresponding author upon request.

References

[1] Cannistrà M, Ruggiero M, Zullo A, Gallelli G, Serafini S, Maria M, *et al*. Hepatic ischemia reperfusion injury: A systematic review of literature and the role of current drugs and biomarkers. *Int J Surg* 2016;33(Suppl 1):S57-S70. doi:10.1016/j.ijsu.2016.05.050, PMID:27255130.

[2] Quesnelle KM, Bystrom PV, Toledo-Pereyra LH. Molecular responses to ischemia and reperfusion in the liver. *Arch Toxicol* 2015;89(5):651-657. doi:10.1007/s00204-014-1437-x, PMID:25566829.

[3] Jiménez-Castro MB, Cornide-Petronio ME, Gracia-Sancho J, Peralta C. Inflammation-Mediated Inflammation in Liver Ischemia-Reperfusion Injury. *Cells* 2019;8(10):1131. doi:10.3390/cells8101131, PMID:31547621.

[4] Xu S, Niu P, Chen K, Xia Y, Yu Q, Liu N, *et al*. The liver protection of propylene glycol alginate sodium sulfate preconditioning against ischemia reperfusion injury: focusing MAPK pathway activity. *Sci Rep* 2017;7(1):15175. doi:10.1038/s41598-017-15521-3, PMID:29123239.

[5] Masior Ł, Grał M. Methods of Attenuating Ischemia-Reperfusion Injury in Liver Transplantation for Hepatocellular Carcinoma. *Int J Mol Sci* 2021;22(15):8229. doi:10.3390/ijms22158229, PMID:34360995.

[6] Van den Bossche J, O'Neill LA, Menon D. Macrophage Immunometabolism: Where Are We (Going)? *Trends Immunol* 2017;38(6):395-406. doi:10.1016/j.it.2017.03.001, PMID:28396078.

[7] Lu X, Liu T, Chen K, Xia Y, Dai W, Xu S, *et al*. Isorhamnetin: A hepatoprotective flavonoid inhibits apoptosis and autophagy via P38/PPAR-α pathway in mice. *Biomed Pharmacother* 2018;103:800-811. doi:10.1016/j.biopha.2018.04.016, PMID:29684859.

[8] Feng J, Wu L, Ji J, Chen K, Yu Q, Zhang J, *et al*. PKM2 is the target of proanthocyanidin B2 during the inhibition of hepatocellular carcinoma. *J Exp Clin Cancer Res* 2019;38(1):204. doi:10.1186/s13046-019-1194-z, PMID:31101057.

[9] Rauf A, Imran M, Abu-Izneid T, Ihtisham Ul H, Patel S, Pan X, *et al*. Proanthocyanidins: A comprehensive review. *Biomed Pharmacother* 2019;116:108999. doi:10.1016/j.biopha.2019.108999, PMID:31146109.

[10] Rodríguez-Pérez C, García-Villanova B, Guerra-Hernández E, Verardo V. Grape Seeds Proanthocyanidins: An Overview of In Vivo Bioactivity in Animal Models. *Nutrients* 2019;11(10):2435. doi:10.3390/nu11102435, PMID:31614852.

[11] Sizlan A, Guven A, Uysal B, Yanarates O, Atim A, Oztas E, *et al*. Proanthocyanidin protects intestine and remote organs against mesenteric ischemia/reperfusion injury. *World J Surg* 2009;33(7):1384-1391. doi:10.1007/s00268-009-0011-9, PMID:19404709.

[12] Wei R, Ding R, Wang Y, Tang L. Grape seed proanthocyanidin extract reduces renal ischemia/reperfusion injuries in rats. *Am J Med Sci* 2012;343(6):452-457. doi:10.1097/MAJ.0b013e31823315f7, PMID:22157385.

[13] Xu ZC, Yin J, Zhou B, Liu YT, Yu Y, Li GQ. Grape seed proanthocyanidin protects liver against ischemia/reperfusion injury by attenuating endoplasmic reticulum stress. *World J Gastroenterol* 2015;21(24):7468-7477.

doi:10.3748/wjg.v21.i24.7468, PMID:26139992.

[14] Yang D, Jiang H, Lu J, Lv Y, Baiyun R, Li S, *et al*. Dietary grape seed proanthocyanidin extract regulates metabolic disturbance in rat liver exposed to lead associated with PPARα signaling pathway. *Environ Pollut* 2018;237:377-387. doi:10.1016/j.envpol.2018.02.035, PMID:29502000.

[15] Holm LJ, Mønsted M, Haupt-Jorgensen M, Buschard K. PPARs and the Development of Type 1 Diabetes. *PPAR Res* 2020;2020:6198628. doi:10.1155/2020/6198628, PMID:32395123.

[16] Kytikova OY, Perelman JM, Novgorodtseva TP, Denisenko YK, Kolosov VP, Antonyuk MV, *et al*. Peroxisome Proliferator-Activated Receptors as a Therapeutic Target in Asthma. *PPAR Res* 2020;2020:8906968. doi:10.1155/2020/8906968, PMID:32395125.

[17] Deng J, Feng J, Liu T, Lu X, Wang W, Liu N, *et al*. Beraprost sodium preconditioning prevents inflammation, apoptosis, and autophagy during hepatic ischemia-reperfusion injury in mice via the P38 and JNK pathways. *Drug Des Devel Ther* 2018;12:4067-4082. doi:10.2147/dddt.518229, PMID:30568428.

[18] Abu About O, Donohoe D, Bultman S, Fitch M, Riiff T, Hellerstein M, *et al*. PPARα inhibition modulates multiple reprogrammed metabolic pathways in kidney cancer and attenuates tumor growth. *Am J Physiol Cell Physiol* 2015;308(11):C890-898. doi:10.1152/ajpcell.00322.2014, PMID:25810260.

[19] Feng J, Zhang Q, Mo W, Wu L, Li S, Li J, *et al*. Salidroside pretreatment attenuates apoptosis and autophagy during hepatic ischemia-reperfusion injury by inhibiting the mitogen-activated protein kinase pathway in mice. *Drug Des Devel Ther* 2017;11:1989-2006. doi:10.2147/dddt.5136792, PMID:28721018.

[20] Wang W, Wu L, Li J, Ji J, Chen K, Yu Q, *et al*. Alleviation of Hepatic Ischemia Reperfusion Injury by Oleoic Acid Pretreatment via Reducing HMGB1 Release and Inhibiting Apoptosis and Autophagy. *Mediators Inflamm* 2019;2019:3240713. doi:10.1155/2019/3240713, PMID:31316298.

[21] Tang J, Lu L, Liu Y, Ma J, Yang L, Li L, *et al*. Quercetin improve ischemia/reperfusion-induced cardiomyocyte apoptosis in vitro and in vivo study via SIRT1/PGC-1α signaling. *J Cell Biochem* 2019;120(6):9747-9757. doi:10.1002/jcb.28255, PMID:30656723.

[22] Bonda TA, Szynaka B, Sokolowska M, Dziemidowicz M, Waszkiewicz E, Winnicka MM, *et al*. Interleukin 6 modulates PPARα and PGC-1α and is involved in high-fat diet induced cardiac lipotoxicity in mouse. *Int J Cardiol* 2016;219:1-8. doi:10.1016/j.ijcard.2016.05.021, PMID:27253588.

[23] Haemmerle G, Moustafa T, Woelkart G, Büttner S, Schmidt A, van de Weijer T, *et al*. ATGL-mediated fat catabolism regulates cardiac mitochondrial function via PPAR-α and PGC-1. *Nat Med* 2011;17(9):1076-1085. doi:10.1038/nm.2439, PMID:21857651.

[24] Nierenberg AA, Ghaznavi SA, Sande Mathias I, Ellard KK, Janos JA, Sylvia LG. Peroxisome Proliferator-Activated Receptor Gamma Coactivator-1 Alpha as a Novel Target for Bipolar Disorder and Other Neuropsychiatric Disorders. *Biol Psychiatry* 2018;83(9):761-769. doi:10.1016/j.biopsych.2017.12.014, PMID:29502862.

[25] Peralta C, Jiménez-Castro MB, Gracia-Sancho J. Hepatic ischemia and reperfusion injury: effects on the liver sinusoidal milieu. *J Hepatol* 2013;59(5):1094-1106. doi:10.1016/j.jhep.2013.06.017, PMID:23811302.

[26] Chouchani ET, Pell VR, Gaude E, Aksentijevic D, Sundier SY, Robb EL, *et al*. Ischaemic accumulation of succinate controls reperfusion injury through mitochondrial ROS. *Nature* 2014;515(7527):431-435. doi:10.1038/nature13909, PMID:25383517.

[27] Cadenas S. ROS and redox signaling in myocardial ischemia-reperfusion injury and cardioprotection. *Free Radic Biol Med* 2018;117:76-89. doi:10.1016/j.freeradbiomed.2018.01.024, PMID:29373843.

[28] Minutoli L, Puzzolo D, Rinaldi M, Irrera N, Marini H, Arcoraci V, *et al*. ROS-Mediated NLRP3 Inflammasome Activation in Brain, Heart, Kidney, and Testis Ischemia/Reperfusion Injury. *Oxid Med Cell Longev* 2016;2016:2183026. doi:10.1155/2016/2183026, PMID:27127546.

[29] Cadenas S. Mitochondrial uncoupling, ROS generation and cardioprotection. *Biochim Biophys Acta Bioenerg* 2018;1859(9):940-950. doi:10.1016/j.bbabi.2018.05.019, PMID:29859845.

[30] Ahmed S, Ahmed N, Rungtatscher A, Linardi D, Kulsoom B, Innamorati G, *et al*. Cocoa Flavonoids Reduce Inflammation and Oxidative Stress in a Myocardial Ischemia-Reperfusion Experimental Model. *Antioxidants (Basel)* 2020;9(2):167. doi:10.3390/antiox9020167, PMID:32085604.

[31] Cao WL, Huang HB, Fang L, Hu JN, Jin ZM, Wang RW. Protective effect of ginkgo proanthocyanidins against cerebral ischemia/reperfusion injury associated with its antioxidant effects. *Neural Regen Res* 2016;11(11):1779-1783. doi:10.4103/1673-5374.194722, PMID:28123420.

[32] Yang B, Sun Y, Lv C, Zhang W, Chen Y. Procyanidins exhibits neuroprotective activities against cerebral ischemia reperfusion injury by inhibiting TLR4-NLRP3 inflammasome signal pathway. *Psychopharmacology (Berl)* 2020;237(11):3283-3293. doi:10.1007/s00213-020-05610-z, PMID:32729095.

[33] Lemberger T, Desvergne B, Wahli W. Peroxisome proliferator-activated receptors: a nuclear receptor signaling pathway in lipid physiology. *Annu Rev Cell Dev Biol* 1996;12:335-363. doi:10.1146/annurev.cellbio.12.1.335, PMID:8970730.

[34] Poulsen L, Siersbæk M, Mandrup S. PPARs: fatty acid sensors controlling metabolism. *Semin Cell Dev Biol* 2012;23(6):631-639. doi:10.1016/j.semcdb.2012.01.003, PMID:22273692.

[35] Bougarne N, Weyers B, Desmet SJ, Deckers J, Ray DW, Staels B, *et al*. Molecular Actions of PPARα in Lipid Metabolism and Inflammation. *Endocr Rev* 2018;39(5):760-802. doi:10.1210/er.2018-00064, PMID:30020428.

[36] González-Mañán D, D'Espessilles A, Dossi CG, San Martín M, Mancilla RA,

- Tapia GS. Rosa Mosqueta Oil Prevents Oxidative Stress and Inflammation through the Upregulation of PPAR- α and NRF2 in C57BL/6J Mice Fed a High-Fat Diet. *J Nutr* 2017;147(4):579–588. doi:10.3945/jn.116.243261, PMID:28298541.
- [37] Chen J, Chen J, Fu H, Li Y, Wang L, Luo S, *et al*. Hypoxia exacerbates nonalcoholic fatty liver disease via the HIF-2 α /PPAR α pathway. *Am J Physiol Endocrinol Metab* 2019;317(4):E710–e722. doi:10.1152/ajpendo.00052.2019, PMID:31430204.
- [38] Kim Y, Park CW. Mechanisms of Adiponectin Action: Implication of Adiponectin Receptor Agonism in Diabetic Kidney Disease. *Int J Mol Sci* 2019;20(7):1782. doi:10.3390/ijms20071782, PMID:30974901.
- [39] Liu GZ, Hou TT, Yuan Y, Hang PZ, Zhao JJ, Sun L, *et al*. Fenofibrate inhibits atrial metabolic remodelling in atrial fibrillation through PPAR- α /sirtuin 1/PGC-1 α pathway. *Br J Pharmacol* 2016;173(6):1095–1109. doi:10.1111/bph.13438, PMID:26787506.
- [40] Sutar I, Sureda A, Belwal T, Sanches Silva A, Vacca RA, Tewari D, *et al*. Natural products, PGC-1 α , and Duchenne muscular dystrophy. *Acta Pharm Sin B* 2020;10(5):734–745. doi:10.1016/j.apsb.2020.01.001, PMID:32528825.
- [41] Sugden MC, Caton PW, Holness MJ. PPAR control: it's SIRTainly as easy as PGC. *J Endocrinol* 2010;204(2):93–104. doi:10.1677/joe-09-0359, PMID:19770177.
- [42] Cordoba-Chacon J. Loss of Hepatocyte-Specific PPAR γ Expression Ameliorates Early Events of Steatohepatitis in Mice Fed the Methionine and Choline-Deficient Diet. *PPAR Res* 2020;2020:9735083. doi:10.1155/2020/9735083, PMID:32411189.
- [43] Kauppinen A, Suuronen T, Ojala J, Kaarniranta K, Salminen A. Antagonistic crosstalk between NF- κ B and SIRT1 in the regulation of inflammation and metabolic disorders. *Cell Signal* 2013;25(10):1939–1948. doi:10.1016/j.cellsig.2013.06.007, PMID:23770291.
- [44] Wang M, Ma LJ, Yang Y, Xiao Z, Wan JB. n-3 Polyunsaturated fatty acids for the management of alcoholic liver disease: A critical review. *Crit Rev Food Sci Nutr* 2019;59(sup1):S116–S129. doi:10.1080/10408398.2018.1544542, PMID:30580553.
- [45] O'Neill KL, Huang K, Zhang J, Chen Y, Luo X. Inactivation of pro-survival Bcl-2 proteins activates Bax/Bak through the outer mitochondrial membrane. *Genes Dev* 2016;30(8):973–988. doi:10.1101/gad.276725.115, PMID:27056669.
- [46] Zhang Y, Yang X, Ge X, Zhang F. Puerarin attenuates neurological deficits via Bcl-2/Bax/cleaved caspase-3 and Sirt3/SOD2 apoptotic pathways in subarachnoid hemorrhage mice. *Biomed Pharmacother* 2019;109:726–733. doi:10.1016/j.biopha.2018.10.161, PMID:30551525.